Vol 15 No 11, November 2006
1009-1963/2006/15(11)/2735-07

Chinese Physics

© 2006 Chin. Phys. Soc.
and IOP Publishing Ltd

Self-consistent analysis of double-δ-doped InAlAs/InGaAs/InP HEMTs

Li Dong-Lin(李东临)† and Zeng Yi-Ping(曾一平)

Novel Materials Laboratory, Institute of Semiconductors, Chinese Academy of Sciences, Beijing 100083, *China*

(Received 31 March 2006; revised manuscript received 5 July 2006)

We have carried out a theoretical study of double-δ-doped InAlAs/InGaAs/InP high electron mobility transistor (HEMT) by means of the finite differential method. The electronic states in the quantum well of the HEMT are calculated self-consistently. Instead of boundary conditions, initial conditions are used to solve the Poisson equation. The concentration of two-dimensional electron gas (2DEG) and its distribution in the HEMT have been obtained. By changing the doping density of upper and lower impurity layers we find that the 2DEG concentration confined in the channel is greatly affected by these two doping layers. But the electrons depleted by the Schottky contact are hardly affected by the lower impurity layer. It is only related to the doping density of upper impurity layer. This means that we can deal with the doping concentrations of the two impurity layers and optimize them separately. Considering the sheet concentration and the mobility of the electrons in the channel, the optimized doping densities are found to be 5×10^{12} and 3×10^{12} cm^{-2} for the upper and lower impurity layers, respectively, in the double-δ-doped InAlAs/InGaAs/InP HEMTs.

Keywords: two-dimensional electron gas, high electron mobility transistor, self-consistent calculation, InAlAs/InGaAs heterostructure

PACC: 7360L, 0200

1. Introduction

The high electron mobility transistors (HEMTs) are devices with potential applications in both microwave and high-speed digital fields due to their superior transport properties.[1−3] Ever since its introduction in the 1980s, several heterostructures (AlGaAs/GaAs, AlGaAs/InGaAs, InAlAs/InGaAs etc) have been studied and a great progress has been made.[4−10] Among them InAlAs/InGaAs heterostructure was found to be more promising than others. Compared with conventional AlGaAs/GaAs HEMTs, the InP-based HEMTs have a larger conduction band discontinuity and a smaller electron effective mass, which allows for higher sheet electron concentration and faster electron saturation velocity.[11−14] Since their first appearance, InP-based HEMTs have become one of the most promising active devices in the high-speed integrated circuits (ICs) and millimetre-wave, microwave ICs.

Normally we want to have higher electron concentration in two-dimensional electron gas (2DEG) because it can provide better power application. In order to further enhance it, double-δ-doped structure is used instead of single-δ-doped structure.[15] In the single-δ-doped HEMT, the ionized electrons from the δ-doped layer were partly transferred to the channel layer, and an electric field was produced between the doped and the channel layers. A quasi-triangle well was formed with a sloping energy band. Obviously, the number of electrons confined in the quantum well is affected by the shape of the well. If the slope angle of the underside of the quantum well is depressed, the position of the subband energy level in the quantum well will be lowered, and the number of electrons confined in it will be increased efficiently.

Double-δ-doped HEMT has been studied theoretically and experimentally.[15−18] The results show that double-δ-doped structure provides electron density higher than the single-δ-doped structure by a factor of 2. Several analytical charge control models[19,20] have been developed to explain the physical mechanism of the device. But some approximations must be used in the process of dealing with the charge control model. This diminishes the creditability when it is used to explain the experimental results. The numerical calculations based on the self-consistent solution of Poisson's and Schrödinger's equations can solve the problem effectively. Several self-consistent methods have been

†E-mail: ldl@red.semi.ac.cn

developed in dealing with the heterojunction and the single-δ-doped HEMTs.[21−23] Among these methods the paper written by Bouzaïene *et al*[21] is the interesting one. He used finite differential method (FDM) to discretize the Schrödinger and Poisson equations, and solve Poisson's equation by using Thomas algorithm under the boundary conditions. In this paper, we apply this self-consistent model to solving the problem of double-δ-doped InAlAs/InGaAs/InP HEMT. The method of solving Poisson's equation is modified by using initial conditions instead of boundary conditions, and the fourth-order Runge–Kutta method is used.

2. Theoretical model

The structure of double-δ-doped HEMT is shown in Fig.1. Lattice-matched HEMT epitaxial layers are grown on semi-insulating InP substrates. The δ-doping layers are located in both barrier layers beside the channel layer. Spacer layers are sandwiched between the channel and the δ-doping layers. On the top layer of the structure a Schottky contact is formed.

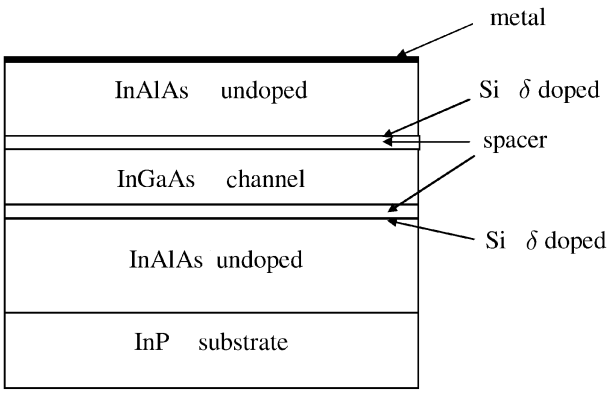


Fig.1. The schematic cross-section of InAlAs/InGaAs HEMT.

Electrons from the doping impurities are transferred to the channel and the metal side of the Schottky contact until a consistent Fermi level is formed. The whole barrier layer is depleted completely. The channel layer acts as a potential well, the width of which is smaller than the de Broglie wavelength; therefore, it is necessary to appeal to the quantum mechanical theory. We assume the validity of the effective mass approximation and take an isotropic and parabolic conduction band in the growth direction. The electron density profiles and electron sheet densities are studied using a self-consistent solution of the Schrödinger and Poisson equations.

The Schrödinger equation is expressed as

$$-\frac{\hbar^2}{2}\frac{\mathrm{d}}{\mathrm{d}z}\Big(\frac{1}{m^*(z)}\frac{\mathrm{d}}{\mathrm{d}z}\Psi_i(z)\Big)+U(z)\,\Psi_i(z)=E_i\,\Psi_i(z), \quad (1)$$

where E_i and Ψ_i are the energy level and wavefunction of the ith subband, respectively, m^* is the position-dependent electron effective mass in the quantization direction (normal to the interface). The potential $U(z)$ can be divided into two different parts:

$$U(z)=U_{\mathrm{b}}(z)+U_{\mathrm{H}}(z), \quad (2)$$

where $U_{\mathrm{b}}(z)$ is the conduction band edge potential without doping and $U_{\mathrm{H}}(z)$ is the electrostatic potential energy.

The electrostatic potential energy is obtained by solving the one-dimensional Poisson equation

$$\frac{\mathrm{d}}{\mathrm{d}z}\Big[\varepsilon(z)\frac{\mathrm{d}}{\mathrm{d}z}U_{\mathrm{H}}(z)\Big]=\frac{e^2}{\varepsilon_0}\Big[N_{\mathrm{d}}(z)-n(z)\Big], \quad (3)$$

where $n(z)$ is the local density of confined electrons and is related to the wavefunctions ψ_i by the following relation

$$n(z)=\sum_i n_i|\,\Psi_i(z)|^2, \quad (4)$$

$$n_i=\frac{m^*k_{\mathrm{B}}T}{\pi\hbar^2}\ln\Big[1+\exp\Big(\frac{E_{\mathrm{F}}-E_i}{k_{\mathrm{B}}T}\Big)\Big]. \quad (5)$$

Here n_i is the occupancy of the ith subband, and E_{F} is the Fermi energy which is constant throughout the system in equilibrium.

The iterative process is used to solve Eqs.(1) and (3) simultaneously until the convergence is completed. The potential energy $U(z)$, the ith subband energy E_i in the quantum well, and the 2DEG concentration are then calculated.

3. Numerical method

In order to solve the Schrödinger equation numerically, we may discretize the differential equation (1) by using the finite-differential method:

$$\begin{aligned}&-\frac{\hbar^2}{\lambda^2}\Big[\Big(\frac{1}{m^*(z_{j-1})+m^*(z_j)}\Big)\Psi_i(z_{j-1})\\&-\Big(\frac{1}{m^*(z_{j-1})+m^*(z_j)}\\&+\frac{1}{m^*(z_j)+m^*(z_{j+1})}\Big)\Psi_i(z_j)\\&+\Big(\frac{1}{m^*(z_j)+m^*(z_{j+1})}\Big)\Psi_i(z_{j+1})\Big]\\&+U(z_j)\,\Psi_i(z_j)=E_i\,\Psi_i(z_j),\end{aligned}$$

$$0 \le j \le M+1 \tag{6}$$

under the boundary conditions of $\Psi_i(z_0) = \Psi_i(z_{M+1}) = 0$, where λ is defined as $\lambda = z_{j+1} - z_j$, $j = 0, 1, \cdots, M+1$.

Equation (6) may be rewritten in the form of matrix equation,

$$\sum_{j=1}^{M} A_{ij}\,\Psi_j = E_i\,\Psi_i, \tag{7}$$

where

$$A_{ij} = \begin{cases} -\dfrac{\hbar^2}{\lambda^2(m^*(z_{i-1}) + m^*(z_i))}, & j = i+1 \\ -\dfrac{\hbar^2}{\lambda^2(m^*(z_{i+1}) + m^*(z_i))}, & j = i-1 \\ \dfrac{\hbar^2}{\lambda^2}\Big(\dfrac{1}{m^*(z_{i-1}) + m^*(z_i)} + \dfrac{1}{m^*(z_i) + m^*(z_{i+1})}\Big), & j = i \\ 0, & \text{otherwise}. \end{cases}$$

This provides a tridiagonal matrix. It is easy to obtain its eigenvalues E_i and its corresponding eigenfunctions Ψ_i.

Firstly, a trial potential $U(z)$ is tested. The wavefunctions and the eigenenergies derived from Eq.(6) can be used to calculate the electron density distribution $n(z)$ by using Eq.(4). If the donor concentration of the two doped layers $N_{\mathrm{d}1}(z)$ and $N_{\mathrm{d}2}(z)$ are given, then the concentration of electrons transferred to the metal side of the Schottky contact will be $(N_{\mathrm{d}1} + N_{\mathrm{d}2} - n_{\mathrm{s}})$, and the electrical field close to the interface of the Schottky contact is

$$E = \frac{N_{\mathrm{d}1} + N_{\mathrm{d}2} - n_{\mathrm{s}}}{\varepsilon_{\mathrm{s}}}.$$

The barrier height Φ_{m} of the Schottky junction is completely determined by the characteristics of InAlAs barrier layer and the metal. We use Φ_{m} and E as the initial conditions to calculate $U_{\mathrm{H}}(z)$ using Eq.(3). In solving the Poisson equation, the fourth-order Runge–Kutta method is used. The problem described above can be reduced as follows:

$$\begin{cases} \dfrac{\mathrm{d}^2 U_{\mathrm{H}}}{\mathrm{d}z^2} = \dfrac{1}{\varepsilon_{\mathrm{s}}}[N_{\mathrm{d}}(z) - n(z)], \\ U_{\mathrm{H}}(0) = \dfrac{\Phi_{\mathrm{m}}}{e}, \quad \dfrac{\mathrm{d}U_{\mathrm{H}}}{\mathrm{d}z}\Big|_{z=0} = -E. \end{cases} \tag{8}$$

By introducing a new variable $R(z) = \mathrm{d}U_{\mathrm{H}}(z)/\mathrm{d}z$ and letting $S(z) = U_{\mathrm{H}}(z)$, the problem of second-order ordinary differential equation (ODE) with initial conditions can be reduced to the one of first-order ODEs with initial conditions.

$$\begin{cases} S' = R, \quad S(0) = \dfrac{\Phi_{\mathrm{m}}}{e}, \\ R' = \dfrac{1}{\varepsilon_{\mathrm{s}}}[N_{\mathrm{d}}(z) - n(z)] = f(z), \quad R(0) = -E, \end{cases} \tag{9}$$

A series of nodes are defined in the region $[z_0, z_m]$:

$$z_0 < z_1 < \cdots < z_n < z_{n+1} < \cdots z_{\mathrm{m}}. \tag{10}$$

Supposing the step is λ, we then have $z_n = z_0 + n\lambda$.

The fourth-order Runge–Kutta solution of Eq.(9) can be written as

$$\begin{cases} S_{n+1} = S_n + pR_n + \dfrac{\lambda^2}{6}(L_1 + L_2 + L_3), \\ R_{n+1} = R_n + \dfrac{\lambda}{6}(L_1 + 2L_2 + 2L_3 + L_4), \end{cases} \tag{11}$$

where

$$\begin{cases} L_1 = f(z_n, S_n, R_n), \\ L_2 = f\Big(z_n + \dfrac{\lambda}{2}, S_n + \dfrac{\lambda}{2}R_n, R_n + \dfrac{\lambda}{2}L_1\Big), \\ L_3 = f\Big(z_n + \dfrac{\lambda}{2}, S_n + \dfrac{\lambda}{2}R_n + \dfrac{\lambda^2}{4}L_1, R_n + \dfrac{\lambda}{2}L_2\Big), \\ L_4 = f\Big(z_n + \lambda, S_n + \lambda R_n + \dfrac{\lambda^2}{2}L_2, R_n + \lambda L_3\Big). \end{cases}$$

Substituting the U_{H}, calculated from Eq.(8), in Eq.(2), the $U'(z)$ can be obtained for the coming iterative cycle. However, to accelerate the convergence speed, actually, a new potential energy $U_{\mathrm{new}}(z) = \alpha U'(z) + (1-\alpha)U_{\mathrm{old}}(z)$ is used in the next iterative process, where α is an adjustable parameter ($0 < \alpha < 1$). Each time the calculation process is carried out, a

new value of the 2DEG concentration (n_s) is obtained. Suppose the change of n_s between two adjacent cycle is expressed as Δn_s. The iterative procedure stops when $\Delta n_s/n_s$ is less than 10^{-5}.

4. Results and discussion

The material parameters needed for a self-consistent calculation should be specified before calculation. The Schottky barrier height (Φ_m) and conduction band offset (ΔE_C) are assumed to be 0.7 and 0.51 eV, respectively. (See Fig.2) The effective electron masses in the barrier and the channel layer are assumed to be $0.0813m_e$ and $0.041m_e$ respectively.[24] The thickness of the channel layer is taken to be 15 nm. The doping densities of the two impurity layers (one is above the channel, the other is under the channel) are the device parameters that need to be optimized. Different δ-doping concentrations are adopted in the upper and the lower doped layers. For the upper doped layer, the electrons coming from the ionized impurities are transported to the Schottky contact and the channel. In order to ensure enough electrons transferred to the channel, the upper δ-doping concentration should be high. As for the lower doped layer, the electrons should be transferred to the quantum well, and no residual electrons should remain in the barrier. So the doping density will be limited. We decide the doping density by the following two points: (a) more electrons, (b) higher mobility. Firstly we try to set the two doping concentrations (N_{d1} and N_{d2}) to be 4.5×10^{12} and 2×10^{12} cm^{-2}, respectively, then we obtain the conduction band structure as well as the subband energy levels as follows:

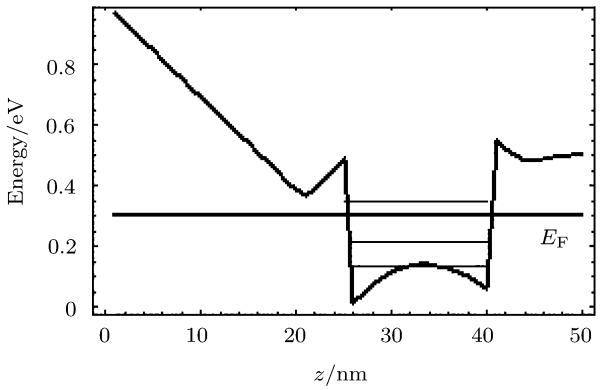


Fig.2. The conduction band structure and the subenergy levels for double δ-doped InAlAs/InGaAs HEMTs.

The wavefunctions subjected to the two lowest subband energy levels are shown in Fig.3:

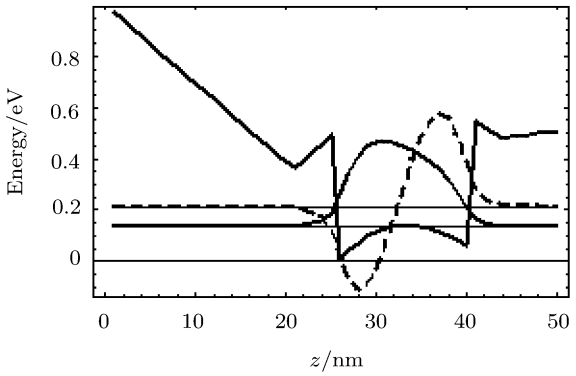


Fig.3. The wavefunction corresponding to the first (soled line) and second (dashed line) subenergy levels.

As mentioned above, the 2DEG is formed by the electrons transferred from both the upper and lower impurity layers. Due to the depletion effect of the Schottky contact, some electrons will transfer to the metal side of the Schottky contact. We have calculated the dependence of sheet electron concentration of 2DEG (n_s) and the number of electrons transferred to the metal of the Schottky contact (n_e) on the doping concentration of upper and lower impurity layers. Figures 4 and 5 show the calculated results.

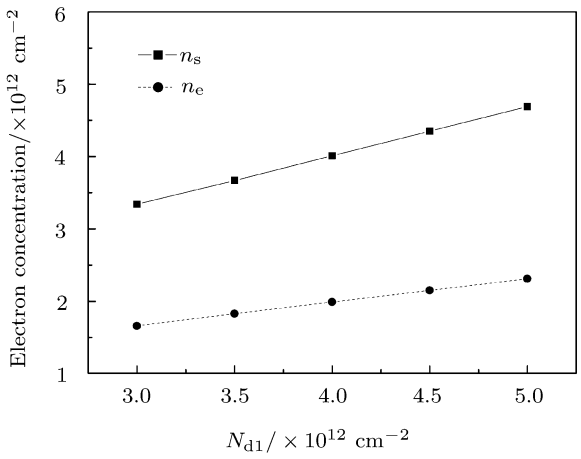


Fig.4. Electron concentration of 2DEG and the electrons transferred to the metal side of the Schottky contact versus doping concentration of the upper impurity layer.

From the figures we find that when the doping density of the upper impurity layer (N_{d1}) increases, the numbers of electrons transferred to the quantum

well and to the metal side of the Schottky contact increase. But when the doping density of the lower impurity layer (N_{d2}) increases, the number of electrons transferred to the metal side of Schottky contact changes slightly. Only the 2DEG concentration changes with it. The number of electrons transferred to the metal side of the Schottky contact determines the electric field inside the barrier layer. Thus it also determines the sloping extent of the conduction band. The above results give us an important revelation that when we want to obtain optimized doping densities of the two layers, we can consider them separately.

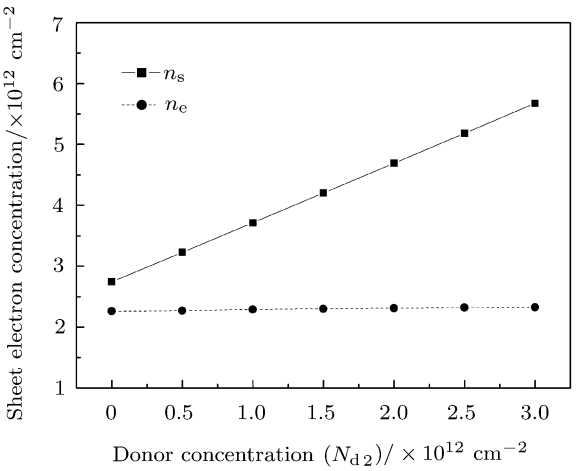


Fig.5. Electron concentration of 2DEG and the electrons transferred to the metal side of the Schottky contact versus doping concentration of the lower impurity layer.

The doping density of upper impurity layer needs to be considered first. Because we want more electrons in the channel layer, we need to improve the doping density as much as possible. But if the number of electrons transferred to the metal side is high enough, the Fermi level will extend across the conduction band, and parallel conduction will occur. Then the characteristics of the device will be damaged. We have calculated the minimum value of the conduction band in the barrier layer and compared them with the Fermi level, as shown in Fig.6. We can find from the figure that when the doping density approaches 5.5×10^{12} cm^{-2}, the minimum value of the conduction band is obviously under the Fermi level. We may set the optimum doping density of the upper impurity as 5.0×10^{12} cm^{-2}. It can provide a maximal value of 2DEG concentration and avoid the appearance of parallel conductance.

The doping density of lower impurity layer can be decided by the following two points: (a) more electrons, (b) higher mobility. We have known that in the case of single-doped structure, the shape of the quantum well is like a quasi-triangle. The centroid of the electrons is much close to the upper interface of the heterojunction, and the electrons will suffer a higher interface roughness scattering. If the electrons are located in the middle of the quantum well and far from the interface of heterostructure, the interface roughness scattering can be depressed effectively.[25−27] The premise of making the electrons (mainly the electrons subjected to the first subenergy level) located in the middle of the quantum well is that the quantum well should become symmetric. When a doped layer is set under the channel, the electrons from the ionized impurities will also transfer to the channel, and an electric field will come into being at this position, then the energy band will be altered by the electric field. Therefore the shape of the quantum well can be adjusted by changing the doping densities of the upper and lower doping layers.

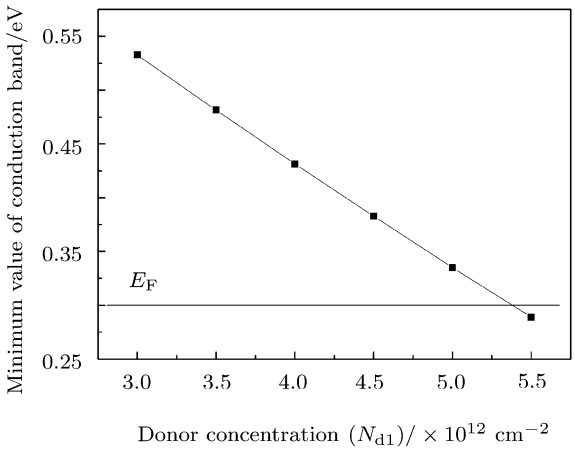


Fig.6. The minimum value of conduction relative to the Fermi level versus donor concentration of upper impurity layer.

After the doping density of the upper impurity layer is determined to be 5.0×10^{12} cm^{-2}, the second impurity layer under the channel is going to be set and its doping density is improved gradually, so that the well is becoming more symmetric and the centroid of the electrons is approaching the middle of the well gradually. At the same time the concentration of 2DEG in the channel improves. This means that while the 2DEG concentration improves, the electrons will suffer less interface roughness scattering, and their

mobility can also be enhanced. Figure 7 shows the band diagram with different N_{d2}. The doping densities of the lower impurity layer are set at 0, 1×10^{12}, 2×10^{12}, 3×10^{12} cm^{-2}. In Fig.7 the distribution of the electrons is also shown. As shown in Fig.2, two subenergy levels exist below the Fermi level. This means that the electrons mainly occupy these two levels, and the local density of electrons is mainly composed of the electrons subjected to these two subenergy levels. We can find from Fig.7 that when the doping densities of the two impurity layers are 5×10^{12} and 3×10^{12} cm^{-2}, respectively, the shape of the band structure is the most symmetrical. Therefore we may expect the best performance of the device in this case, with the electron concentration of 2DEG calculated to be 5.68×10^{12} cm^{-2}. Compared with that of single-doped structure, the 2DEG concentration of double δ-doped HEMT has doubled. The higher electron concentration ensures this HEMT to be a good candidate for high power application. We also expect a better performance of transport properties in this structure.

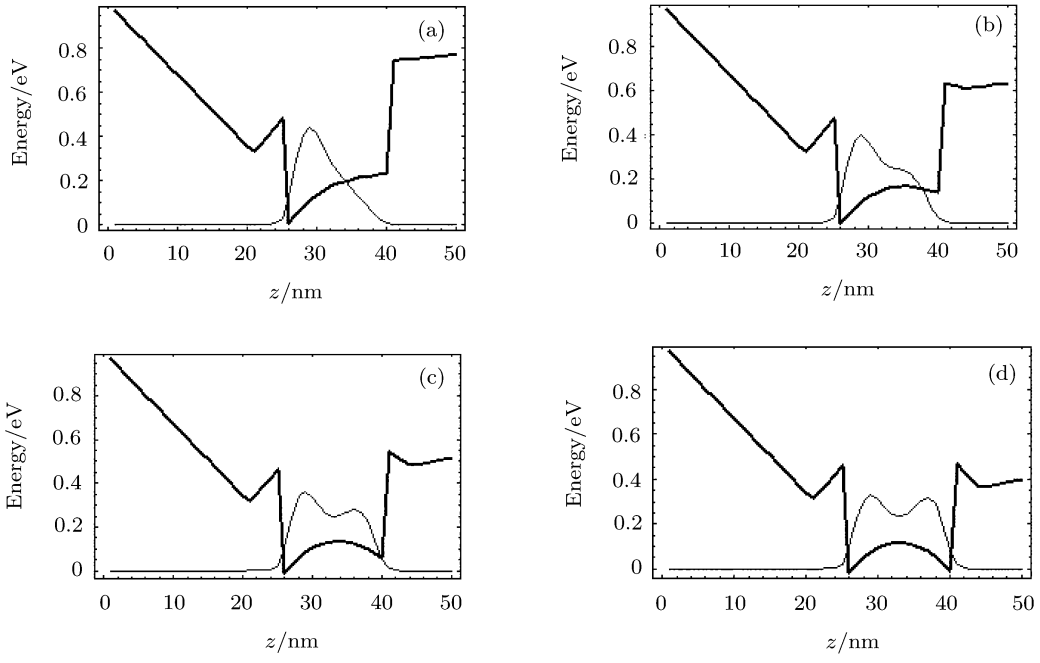


Fig.7. The distribution of electrons in the lower impurity layer with different doping density. For Figs.7(a), 7(b), 7(c) and 7(d) the doping densities are 0, 1×10^{12}, 2×10^{12} and 3×10^{12} cm^{-2}.

5. Conclusion

A theoretical study (self-consistent calculation of the Schrödinger and Poisson equations) has been carried out to determine the properties of the 2DEG in double-δ-doped InAlAs/InGaAs/InP HEMT. The electronic states in the quantum well of the HEMT is calculated. Eigenvalues and corresponding wavefunctions have been obtained by using finite differential method. We have also obtained the sheet electron concentration of 2DEG and its distribution in the quantum well. By changing the doping densities of upper and lower impurity layers, we find that both the 2DEG concentration and the electrons transferred to the metal side of the Schottky contact increase along with the doping concentration of upper impurity layer, but only the 2DEG concentration changes with that of the lower impurity layer. Thus we can optimize the doping concentrations of two layers separately. Considering the sheet concentration and the mobility of the electrons, the optimum doping concentrations for the two layers are 5×10^{12} and 3×10^{12} cm^{-2}, respectively. The result of 2DEG concentration has been compared with that of single-δ-doped HEMT, and we find that the 2DEG concentration has doubled. So we

can conclude that it is a very good candidate for power application. We believe these results can provide important information for designing double-doped InAlAs/InGaAs/InP HEMTs.

References

[1] Aust M, Wang H, Biedenbender M, Lai R, Streit D C, Liu P H, Dow G S and Allen B R 1995 *IEEE Microwave Guid. Wave Lett.* **5** 12

[2] Grundbacher R, Ketterson A A, Kao Y C and Adesida I 1997 *IEEE Trans. Electron Devices* **44** 2136

[3] Wu C S, Ren F, Pearton S J, Hu M, Pao C K and Wang R F 1995 *IEEE Trans. Electron Devices* **42** 1419

[4] Delagebeaudeuf D and Linh N T 1982 *IEEE Trans. Electron Devices* **29** 955

[5] Drummond T J, Morkoc H, Lee K and Shur M 1982 *IEEE Electron Device Lett.* **3** 338

[6] Sen S, Pandey M K and Gupta R S 1999 *IEEE Trans. Electron Devices* **46** 1818

[7] Rohdin H and Roblin P 1986 *IEEE Trans. Electron Devices* **33** 664

[8] Ahn H and Nokali M 1994 *IEEE Trans. Electron Devices* **41** 874

[9] Qiu Z J, Jiang C P, Gui Y S, Shu X Z, Guo S L, Chu J H, Cui L J, Zeng Y P, Zhu Z P and Wang B Q 2003 *Acta Phys. Sin.* **52** 2879 (in Chinese)

[10] Liu H X, Hao Y, Zhang T, Zheng X F and Ma X H 2003 *Acta Phys. Sin.* **52** 984 (in Chinese)

[11] Hong W P, Bhat R, Hayes J R, Nguyen C and Chang G K 1991 *IEEE Electron Device Lett.* **12** 559

[12] Xu D, Suemitsu T, Osaka J, Umeda Y, Yamane Y, Ishii Y, Ishii T and Tamamura T 1999 *IEEE Electron Device Lett.* **20** 206

[13] Maher H, Decobert J, Falcou A, Pallec M L, Post G, Nissim Y I and Scavennec A 1999 *IEEE Trans. Electron Devices* **46** 32

[14] Kusters A M, Kohl A, Muller R, Sommer V and Heime K 1993 *IEEE Electron Device Lett.* **14** 36

[15] Cazaux J L, Ng G I, Pavlidis D and Chau H F 1988 *IEEE Trans. Electron Devices* **35** 1223

[16] Inoue K, Sakaki H, Yoshino J and Hotta T 1985 *J. Appl. Phys* **58** 4277

[17] Gupta R, Aggarwal S K, Gupta M and Gupta R S 2005 *Solid-State Electronics* **49** 167

[18] Tan K L, Streit D C, Dia R M, Wang S K, Han A C, Chow P-M D, Trinh T Q, Liu P H, Velebir J R and Yen H C 1991 *IEEE Electron Device Lett.* **12** 213

[19] Lien C H, Huang Y M, Chien H M and Wang W L 1994 *IEEE Trans. Electron Devices* **41** 1351

[20] Chen Z, Liu X Y and Wu D X 2004 *Chin. J. Semiconductors* **25** 836

[21] Bouzaïene L, Sfaxi L, Sghaeir H and Maaref H 1999 *J. Appl. Phys.* **85** 8223

[22] Tan I H, Snider G L, Chang L D and Hu E L 1990 *J. Appl. Phys.* **68** 4071

[23] Halkias G, Vegiri A, Pananakakis G and Christou A 1992 *Solid-State Electronics* **35** 459

[24] Vurgaftman I, Meyer J R and Ram-Mohan L R 2001 *J. Appl. Phys.* **89** 5815

[25] Li Y J, Hsu W C, Chen I L, Lee C S, Chen Y J and Lo I 2004 *J. Vac. Sci. Technol. B.* **22** 2429

[26] Xu D, Heiβ H G, Kraus S A, Sexl M, Böhm G, Tränkle G and Weimann G 1997 *IEEE Electron Device Lett.* **18** 323

[27] Xu D, Heiβ H G, Kraus S A, Sexl M, Böhm G, Tränkle G and Weimann G 1998 *IEEE Trans. Electron Devices* **45** 21